Available online at www.sciencedirect.com
SCIENCE DIRECT
Journal of Catalysis 235 (2005) 413–422
JOURNAL OF CATALYSIS
www.elsevier.com/locate/jcat

A spectroscopy and catalysis study of the nature of active sites of MgO catalysts: Thermodynamic Brønsted basicity versus reactivity of basic sites

Marie-Laurence Bailly [a], Céline Chizallet [a], Guylène Costentin [a], Jean-Marc Krafft [a], Hélène Lauron-Pernot [a,*], Michel Che [a,b]

[a] *Laboratoire de Réactivité de Surface, UMR 7609 CNRS, Université Pierre et Marie Curie, 4 place Jussieu, 75252 Paris cedex 05, France*
[b] *Institut Universitaire de France, France*

Received 13 April 2005; revised 8 August 2005; accepted 4 September 2005

Abstract

The relationship between thermodynamic Brønsted basicity and reactivity of basic sites of MgO samples was investigated by means of methanol deprotonation followed by IR and the conversion of 2-methylbut-3-yn-2-ol (MBOH), respectively. The relative distribution of basic oxide ions, O^{2-}_{LC}, in low coordination (where LC = 3C, 4C, and 5C refer to tri-, tetra-, and penta-coordinated oxide ions, respectively) was modulated using different preparation routes. The resulting samples were classified on the basis of the relative distributions of O^{2-}_{LC} ions determined by photoluminescence. The influence of the coordination of O^{2-}_{LC} ions on the basic properties was studied for clean surfaces obtained after high-temperature ($\geqslant$1023 K) evacuation of CO_2 and water; the lower the coordination of O^{2-}_{LC} ions, the higher the deprotonation ability and the reactivity of basic sites of the catalyst. The hydroxylation of clean MgO surfaces was studied and its influence on Brønsted basicity determined. Despite a low deprotonation ability, hydroxylated surfaces are more reactive than clean surfaces. The direct influence of OH groups on reactivity of basic sites was evidenced by correlating the latter and the amount of isolated OH groups evaluated by in situ diffuse reflectance Fourier transform infrared spectroscopy. It can be inferred that the peculiar reactivity of OH groups compared with O^{2-}_{LC} ions is due to the variable stability of the alcoholate intermediate formed on both kinds of basic sites. On hydroxylated surfaces, because OH groups are poor Brønsted bases, the number of alcoholate species is lower than on clean surfaces, but these intermediates are less stabilized and so are more reactive.

Keywords: Basicity; MgO; Surface; Methylbutynol conversion; Oxide ion; Hydroxyls; Coordination; FTIR; Diffuse reflectance; Photoluminescence; Spectroscopy; Catalysis; Active site

1. Introduction

In the field of heterogeneous catalysis, many reactions involve the acido–basic properties of the catalyst surface. The characterization of acid sites has been much studied. In contrast, because of the limited use of solid bases in industry [1], the notion of basicity has been less well studied, although interest in solid bases has been growing since the 1970s [2]. Their applications, ranging from alkene isomerization to fine chemistry, have been reviewed [3–5]. Surprisingly, the first question that can be asked concerning the characterization of solid base catalysts is how a solid base can be recognized. Hattori [4] gave four criteria, summarized as follows:

(a) Existence of an interaction between the basic surfaces sites and acidic probe molecules;
(b) Existence of a correlation between catalytic activity and number and strength of basic sites or poisoning of active sites by acidic molecules;
(c) Behaviour of the material similar to that of well-known homogeneous basic catalysts;
(d) Evidence that anionic intermediates are involved in the reaction.

* Corresponding author. Fax: +33 01 44 27 60 33.
E-mail address: pernot@ccr.jussieu.fr (H. Lauron-Pernot).

0021-9517/$ – see front matter
doi:10.1016/j.jcat.2005.09.004

In fact, most studies [4,6] report correlations between the basic properties of the surface estimated by the adsorption of a probe molecule (criterion a) and the ability to react along a basic route (criteria b, c, and d), which can be referred to as reactivity of basic sites and can be evaluated by the reaction rate, that is, the catalytic activity.

From our point of view, such attempts raise some questions. First, the interaction of probe molecules (like carbon dioxide) chosen to be observed by spectroscopy [7] or followed by thermodesorption techniques [8] is generally nondissociative and used to evaluate the ability of the surface to share an electron pair, hence its Lewis basicity.

However, the reactivity of basic sites defined by criterion d implies a deprotonation step in which the catalyst behaves as a Brønsted base. Are these two kinds of basicity necessarily correlated? Recall Brønsted's original definition [9]: "der chemische Charakter der Saüren und Basen ist am einfachsten und allgemeinsten durch das Schema:

$$\text{Saüre} \rightleftharpoons \text{Base} + \text{H}^+$$

definiert. Das Hydroxylion nimmt prinzipiell keine Sonderstellung als Träger der basischen Eigenschaften ein." A Brønsted base was thus defined as a species able to protonate itself but is not necessarily an hydroxyl anion. Thus a Lewis basic site, typically an oxide ion, can also behave as a Brønsted basic site, but its deprotonating power, which is distinct from its ability to share an electron pair, implies stabilization of the anionic deprotonated entity.

Second, the basic thermodynamic basic properties of the surface are determined by the position of the adsorption equilibrium or by the energy of interaction of the oxide surface with an acidic probe molecule. Are the latter always related to the activity of a catalytic reaction known to proceed via a basic mechanism?

To answer these questions, MgO materials were chosen because they are well-known basic catalysts [4] and were previously studied in our laboratory [10–12]. As proposed earlier [13], different Mg–O pairs exist at the surface of MgO, where Mg^{2+} and O^{2-} ions have different coordination numbers depending on their location (terrace, corner, or edge). The basic sites are generally considered to be oxide ions of low coordination, denoted by O^{2-}_{LC} (where LC = 3C, 4C, and 5C refer to tri-, tetra-, and penta-coordinated oxide ions, respectively). Usually the influence of the nature of the basic site is studied by treating the samples at increasing temperature to remove contaminants, progressively leading to stronger basic sites. However, the influence of the remaining adsorbates in the vicinity of the O^{2-}_{LC} ions liberated, inherent to such a procedure, cannot be neglected. Moreover, such thermal treatments lead to surface reconstructions, thus modifying the relative distribution of O^{2-}_{LC} ions [4].

Our approach has been to vary the relative distribution of O^{2-}_{LC} ions by means of the preparation routes. As described earlier [11,12], the relative distribution of O^{2-}_{LC} ions is determined by photoluminescence spectroscopy, one of the few techniques able to discriminate O^{2-}_{LC} ions [14]. The stability of the surfaces versus thermal treatment can be evaluated by comparing the spectra obtained before and after treatment. The nature of the basic sites can also be changed by hydroxylation of the surface, because basic hydroxyl groups are known to promote some basic reactions [15,16]. The aim of this work is to study, on these MgO surfaces, the relation between thermodynamic Brønsted basicity, evaluated by deprotonation ability, and reactivity of basic sites versus the nature of basic site involved.

The thermodynamic Brønsted basicity of dehydroxylated samples has been studied by photoluminescence on protonation of O^{2-}_{LC} ions by propyne [11]. The Brønsted basicity of O^{2-}_{LC} ions was found to increase along the series $O^{2-}_{5C} < O^{2-}_{4C} < O^{2-}_{3C}$. To evaluate the thermodynamic Brønsted basicity of MgO samples in the same treatment conditions as those used for the catalytic reaction, the deprotonation of methanol has been studied on such surfaces by infrared spectroscopy.

The reactivity of basic sites of MgO has been evaluated by means of the conversion of 2-methylbut-3-yn-2-ol (MBOH). This catalytic reaction, proposed to avoid controversial interpretations arising from the use of secondary alcohols [17], is often used to characterise the acid–base properties of catalysts [Lauron-Pernot in preparation]. The use of a catalytic probe reaction is generally thought to be the best tool for revealing the acid–base properties of a solid in real catalytic conditions. The pathways for MBOH reaction are shown in Fig. 1. On acidic

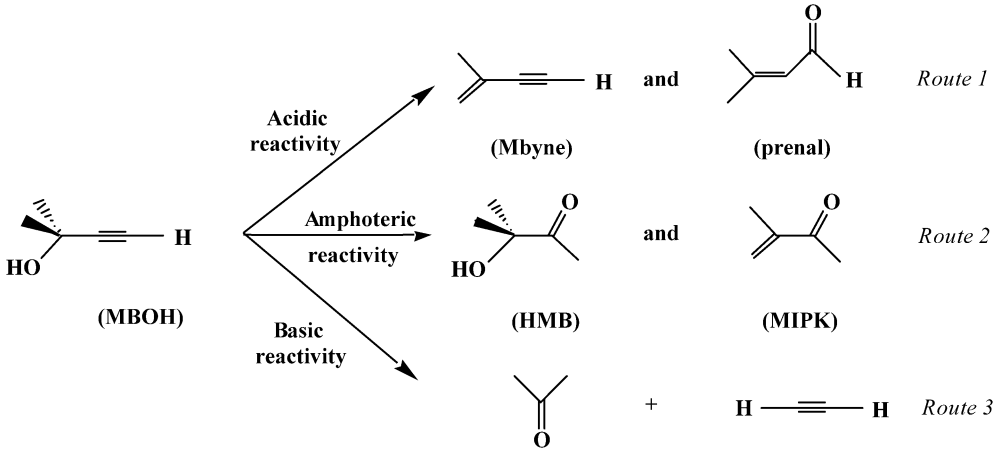

Fig. 1. Reaction pathways of MBOH conversion depending on the nature of catalytic sites [17].

catalysts, MBOH undergoes both dehydration and isomerisation to yield 2-methylbut-1-en-3-yne (Mbyne) and 3-methylbut-2-enal (prenal), respectively; on basic surfaces, MBOH leads to acetone and acetylene. MBOH may also probe amphoteric catalysts by hydration to 3-hydroxy-3-methylbutan-2-one (HMB) and isomerisation to 3-methylbut-3-en-2-one (MIPK). On MgO, the only route observed is the basic one, so that basicity can be evaluated simply by the level of MBOH conversion.

2. Experimental

2.1. Sample preparation

Four samples were studied: MgO-sol–gel, MgO-precipitation, MgO-hydration, and MgO-CVD, so named according to the preparation method, as described earlier [12]. MgO-sol–gel, MgO-precipitation, and MgO-hydration were obtained by treatment under dynamic vacuum (around 0.13 Pa) at 1273 K for 2 h of the corresponding hydroxides. $Mg(OH)_2$-sol–gel was prepared from the hydrolysis of magnesium methanolate. $Mg(OH)_2$-precipitation was formed by the action of aqueous ammonia on magnesium nitrate. $Mg(OH)_2$-hydration was obtained by stirring a commercial MgO (Aldrich, 99.99%) in water for 24 h at room temperature. MgO-CVD, kindly provided by Knözinger [18,19], was obtained through chemical vapor deposition by oxidizing metallic magnesium in a flow of oxygen/argon.

2.2. Specific surface area measurement

The specific surface area and the pore volume of the solids were determined using an automatic porosimeter (Micromeritics ASAP 2010). The samples were outgassed at 473 K for 15 h and then at 573 K for 2 h before measuring the adsorption of nitrogen. The specific surface areas were evaluated by the BET method.

2.3. Sample treatment

2.3.1. Hydroxylation treatment

A 20 mg sample was treated for 1 h at 1023 K under nitrogen (70 $cm^3\,min^{-1}$). Once cooled to 373 K, the sample was treated for 10 min with water vapour (about 840 Pa) diluted in nitrogen (10 $cm^3\,min^{-1}$). Finally, it was heated (5 $K\,min^{-1}$) under nitrogen (70 $cm^3\,min^{-1}$) up to the selected activation temperature and maintained at this temperature for 15 min. This treatment led to the so-called "hydroxylated" surfaces and was used in situ in the diffuse reflectance Fourier transform infrared (DRIFT) cell or in the MBOH reactor.

2.3.2. High-temperature treatment

A high-temperature (1023–1273 K) in situ treatment was used to remove water and carbon dioxide, producing the so-called "clean" surfaces. The highest possible temperature was determined by the heat resistance of the experimental setup specific to each characterization technique and is described below. Only dried gases were used during these treatments, to avoid hydration.

2.4. DRIFT

DRIFT spectra were recorded on a Brüker IFS 66 V spectrometer in the 3800–600 cm^{-1} range (4 cm^{-1} resolution, 256 scans/spectrum) using a Thermo Spectra-Tech high-temperature cell. All spectra were converted into Kubelka–Munk units after subtraction of the spectrum of a KBr sample dehydrated at 473 K under nitrogen (70 $cm^3\,min^{-1}$) for 2 h. The high-temperature in situ treatment consisted of an activation under nitrogen (70 $cm^3\,min^{-1}$) at the highest temperature attainable with this apparatus, that is, 1023 K (5 $K\,min^{-1}$) for 2 h.

2.5. Methanol adsorption followed by transmission IR

Transmission IR spectra were recorded on a Nicolet 750 spectrometer equipped with a DTGS detector (2 cm^{-1} resolution, 64 scans/spectrum). Between 20 and 30 mg of MgO powder was pressed into a self-supporting pellet under 10^6 Pa. The clean surface was obtained by activation under vacuum for 6 h at 673 K, then to 1023 K for 1 h under 1.33×10^4 Pa of oxygen, then under vacuum (final residual pressure of $\approx 6 \times 10^{-4}$ Pa) at 1023 K, the highest possible temperature reached with this apparatus. Hydroxylation of the clean surface was performed on introduction in the cell of 133 Pa of water at 373 K for 10 min. The pellet was then activated at $\approx 6 \times 10^{-4}$ Pa and 673 K for 1 h.

Small aliquots of methanol were introduced on the sample before or after hydroxylation, at ambient temperature so as to reach a final residual pressure of 133 Pa in the cell. The spectrum of the gas phase was subtracted from the spectrum of the sample.

2.6. Methylbutynol reaction

MBOH reaction was followed in an automated differential-flow microreactor. For each experiment, 20 mg of catalyst was pressed into wafers under a pressure of 5×10^5 Pa and crushed into pellets of 125–200 μm diameter. The sample was deposited on porous glass, in the centre of a 10 mm-i.d. U quartz tube. The reaction temperature of 393 K was controlled within ±1 K by a thermocouple located by the catalyst. The desired MBOH partial pressure was obtained by bubbling nitrogen (100 $cm^3\,min^{-1}$) in liquid MBOH at the selected temperature. Reaction products were analysed every 120 s using a Varian micro gas chromatograph equipped with a catharometric detector and a CP WAX 52 CB column.

2.6.1. Standard run

In a standard run, the sample was first subjected to a high-temperature treatment leading to clean surfaces consisting of in situ activation under nitrogen (70 $cm^3\,min^{-1}$) at 1073 K (5 $K\,min^{-1}$) for 2 h in the reactor. The sample was then cooled to 393 K, and MBOH diluted in nitrogen was introduced at a partial pressure of 1.73 kPa by adjusting the saturator temperature to 293 K. The catalytic reaction was then performed at 393 K as described earlier. These conditions were used when

the conversion was such as to ensure the absence of diffusional limitations.

2.6.2. Isosurface area experiments on clean surface

Because samples have different specific surface areas, it is not possible to compare their catalytic activities in the same conditions without being limited by diffusional phenomena. Isosurface area experiments have thus been performed adapting the mass of catalyst so as to obtain a surface of 5 m^2 in the reactor. The constant loading of the reactor was obtained by diluting MgO with SiC (Prolabo, 250 µm diameter) so as to finally reach 75 mg of solid. It has been checked that SiC alone does not convert MBOH. To avoid diffusional problems for all samples, the partial pressure of MBOH was adjusted to 3.3 kPa by increasing the saturator temperature to 303 K. The nitrogen flow was maintained at 70 $cm^3\,min^{-1}$.

2.6.3. Conversion and selectivity

Because acetone and acetylene are the only products detected, catalytic data are expressed in terms of conversion only. The partial pressure of each product P_i was calculated from chromatographic measurements using the appropriate response coefficient and the value of the initial partial pressure of MBOH in the feed, P^0_{MBOH}. The conversion τ is given by

$$\tau\ (\%) = \frac{\sum_{i\neq \mathrm{MBOH}} \alpha P_i}{P^0_{\mathrm{MBOH}}},$$

with $\alpha = 1/2$ for acetone and acetylene. Selectivities in acetone and acetylene are given by

$$S_i\ (\%) = \frac{\frac{1}{2} P_i}{\sum_{i\neq \mathrm{MBOH}} \alpha P_i}.$$

3. Results

3.1. Surface oxide morphology

Table 1 gives, as described earlier [12], the textural and morphological properties of the four MgO samples studied, as well as the relative distribution of O^{2-}_{LC} ions determined by photoluminescence after treatment under dynamic vacuum at 1273 K for 2 h [11,12]. The $O^{2-}_{3\mathrm{C}}$ ions excited at 270 nm emit at 460 nm, whereas the $O^{2-}_{4\mathrm{C}}$ ions excited at 230 nm emit at 380 nm. The ratio of integrated areas of the excitation bands reported in Table 1, is equal to $\alpha O^{2-}_{3\mathrm{C}}/O^{2-}_{4\mathrm{C}}$, where α is a constant. The position of the emission band of $O^{2-}_{4\mathrm{C}}$ ions is also given in Table 1. The shift of this position from 380 nm to a lower wavelength is linked either to direct contribution of $O^{2-}_{5\mathrm{C}}$ [12] or to emission of $O^{2-}_{4\mathrm{C}}$ located on extended defect-free edges [R. Hacquart, Surf. Sci., in press]. In both cases, it probes the relative abundance of $O^{2-}_{5\mathrm{C}}$ ions located on extended (100) planes; the lower the wavelength, the higher the $O^{2-}_{5\mathrm{C}}$ relative abundance.

The MgO samples differ, particularly in their relative distribution of O^{2-}_{LC} ions. MgO-sol–gel has a rough surface, probably due to defects created by desorption of the last residual methoxy groups introduced during synthesis [20]. MgO-hydration and MgO-precipitation exhibit very similar characteristics but for morphology and particle size. The values obtained for MgO-hydration differ from those published earlier [12], indicating that the preparation method is not easily reproducible. Indeed, rehydration of commercial MgO strongly affects the corners of the particles, and the erosion process is not yet well understood [21,22]. MgO-CVD exhibits a very high surface area but, because of its cubic particles, involves O^{2-}_{LC} ions with higher coordination than for the other samples.

Thus, on the basis of photoluminescence data, the relative distribution of O^{2-}_{LC} ions is shifted toward the less coordinated O^{2-}_{LC} ions along the series MgO-CVD < MgO-hydration ≈ MgO-precipitation < MgO-sol–gel.

3.2. Typical catalytic activity of MgO on clean surface

The DRIFT spectrum of MgO-precipitation is shown in Fig. 2 before and after high temperature treatment (1023 K for 2 h under nitrogen) in the DRIFTS cell. It is seen that this treatment removes carbonates (1300–1500 cm^{-1}), leaving only some residual OH groups (3720 cm^{-1}). The MgO samples thus can be considered to exhibit a clean surface and even more so for MgO treated in the catalytic cell at 1073 K. Fig. 3 gives the conversion and selectivity obtained in a standard run for MgO-precipitation; only acetone and acetylene are produced in equimolar ratio, and the conversion versus time on stream is very stable. The carbon balance between the converted reactant

Table 1
Texture, morphology and populations of the O^{2-}_{LC} ions of MgO samples (reproduced from [12])

Sample	Shape of the particles[a]	BET surface area[b] ($m^2\,g^{-1}$)	Particle size[c] (Å)	$\alpha\cdot O^{2-}_{3\mathrm{C}}/O^{2-}_{4\mathrm{C}}$ [d]	$\lambda_{\max}$ (nm) of $O^{2-}_{4\mathrm{c}}$ ions[e]
MgO-sol–gel	Irregular	150	87	0.15	380
MgO-precipitation	Irregular	198	75	0.06	380
MgO-hydratation	Cubic	150	159	0.06	378
MgO-CVD	Cubic	300	70	0.05	370

[a] Determined from transmission electron microscopy graphs.
[b] After preparation (Section 2.1), the samples are left in air. Before N_2-adsorption measurements, they are outgassed at 473 K for 15 h and then at 573 K for 2 h (Section 2.2).
[c] Estimated from X-ray diffraction patterns.
[d] Obtained from photoluminescence experiments. α is a constant.
[e] Obtained from photoluminescence experiments. The excitation wavelength is 230 nm.

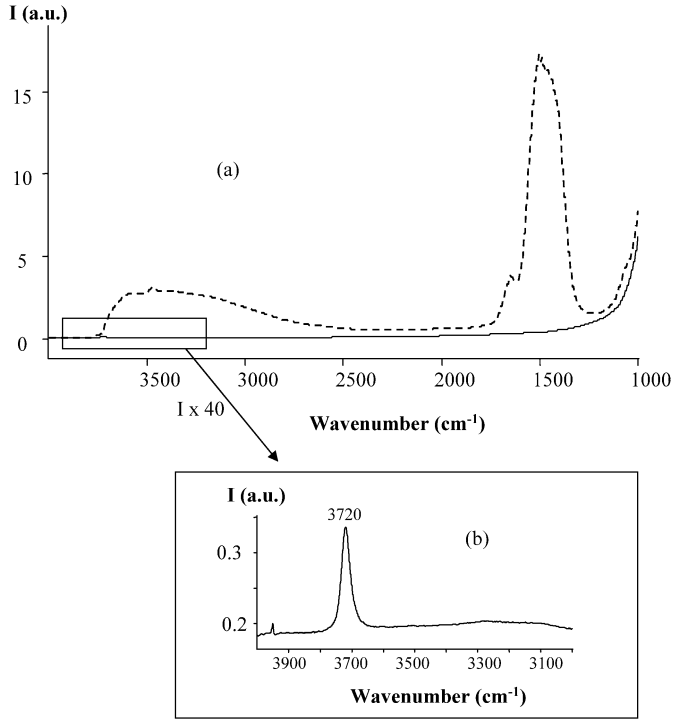

Fig. 2. DRIFT spectra of MgO-precipitation: (a) before activation treatment (- - -) and after activation under nitrogen flow (70 $cm^3\ min^{-1}$) at 1023 K for 2 h (—); (b) after activation under nitrogen flow (70 $cm^3\ min^{-1}$) at 1023 K for 2 h, with zoom on the 3000–4000 cm^{-1} region.

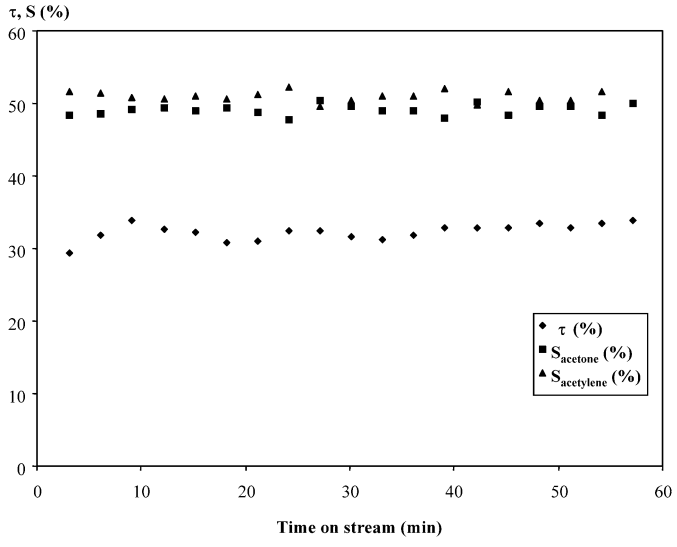

Fig. 3. Conversion and selectivity obtained in a standard run of MBOH reaction on MgO-precipitation as a function of time on stream.

and the products is estimated at >90%. A similar behavior is observed for the other samples.

3.3. Comparison of the activity of basic sites of MgO samples

In isosurface area conditions, the conversions of the different samples are directly linked to the number/m^2 and strength of basic sites. The order of activity thus obtained is MgO-CVD < MgO-precipitation < MgO-hydration < MgO-sol–gel, corresponding to mean conversion values of 23, 15, 12, and 7%, respectively.

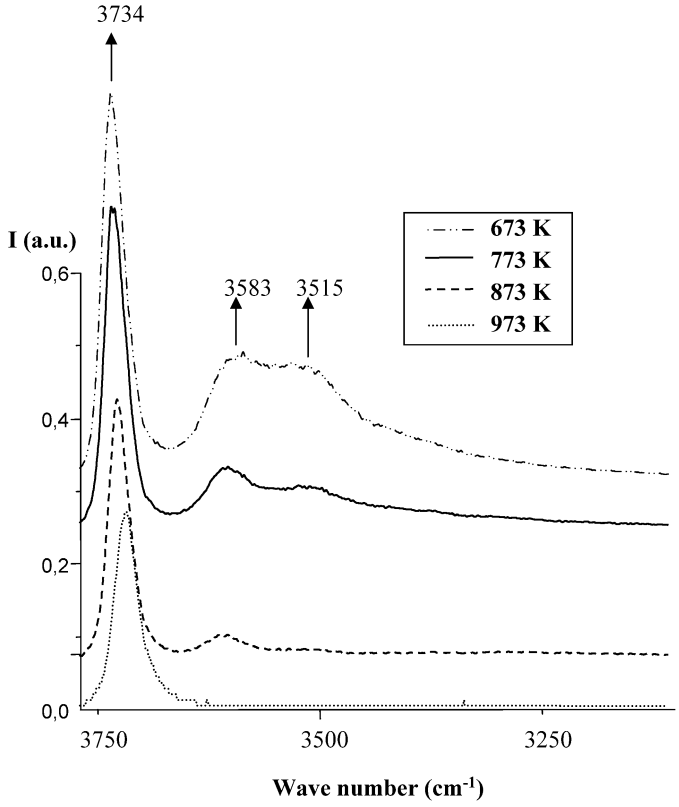

Fig. 4. DRIFT spectra of MgO-precipitation in the ν_{OH} vibration region after each hydroxylation step. Water is adsorbed at 373 K and the sample is heated under nitrogen flow (70 $cm^3\ min^{-1}$) at the desired activation temperature and maintained at this temperature for 15 min. DRIFT spectra are taken at the activation temperature at the end of the dwell.

3.4. Relation between catalytic activity and number of OH groups

3.4.1. Surface hydroxylation followed by DRIFTS

To evaluate the role of OH groups in reactivity of basic sites, the hydroxylation of clean surfaces has been studied. After treatment with water (see Experimental section), the temperature of the sample is increased under flowing nitrogen in 100 °C steps to progressively eliminate physisorbed water and OH groups. Fig. 4 shows the DRIFT spectra in the ν_{OH} region obtained on MgO-precipitation after 15 min at each temperature. They consist of two bands, a broad one around 3500–3650 cm^{-1} and a narrow band around 3700–3750 cm^{-1}. The first is usually assigned to OH groups associated by H-bonding, whereas the second corresponds to isolated OH groups [23–25]. By increasing the desorption temperature, the intensity of the two bands decreases, and at 973 K, only isolated OH groups remain. The area of the two bands measured after subtraction of the background decreases with increasing temperature, as shown in Fig. 5.

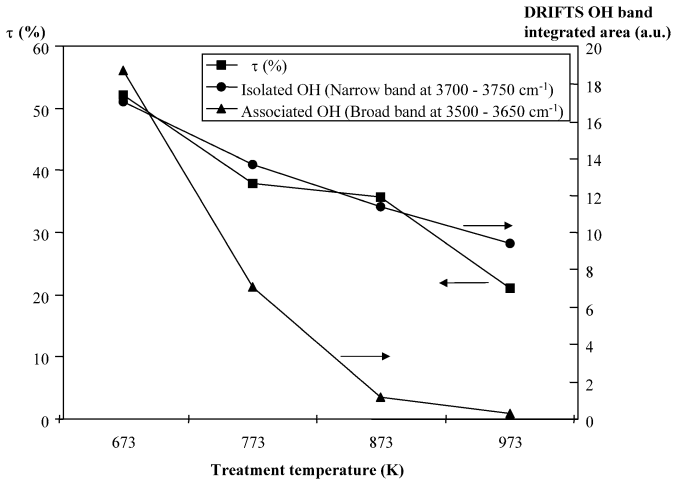

Fig. 5. Evolution of MBOH conversion and of the integrated area of two ν_{OH} DRIFTS bands corresponding respectively to the isolated groups (ν_{OH} = 3700–3750 cm^{-1}) and to the associated groups (ν_{OH} = 3500–3650 cm^{-1}) on MgO-precipitation as a function of treatment temperature.

3.4.2. Catalytic activity of hydroxylated surfaces

The catalytic properties of MgO-sol–gel, MgO-precipitation, and MgO-hydration, treated in the same conditions as those described for DRIFT experiments, were determined. MgO-CVD was not tested in these conditions, because the cubic particles are eroded on rehydration treatment (TEM results not shown) with modification of the O^{2-}_{3C}/O^{2-}_{4C} ratio evidenced by photoluminescence [10,12]. Fig. 5 shows the evolution of conversion τ and of the integrated area of the two ν_{OH} bands with treatment temperature for MgO-precipitation. The same evolution is observed only for τ and the area of the ν_{OH} band corresponding to isolated OH groups. The same result is obtained for MgO-sol–gel and MgO-hydration, suggesting that isolated OH groups play a major role in the reaction. A similar conclusion can be drawn from comparison of conversions in isosurface area conditions of the same MgO-precipitated sample after pretreatment at 1273 K for 2 h under flowing nitrogen (clean surface) (i.e., 15%) and after hydroxylation at 373 K and further dehydroxylation at 673 K for 15 min under flowing nitrogen (i.e., 57.6%).

3.5. Adsorption of methanol followed by transmission IR

The deprotonating ability of MgO surfaces was studied by methanol-IR experiments. Methanol gives simpler spectra than methylbutynol, because the alcoholate formed does not react in the conditions of IR experiments. Earlier results on adsorption of methanol on MgO [26,27] show that different species can be identified by studying the ν_{CO} region (1000–1150 cm^{-1}). Fig. 6 shows the spectrum obtained for MgO-hydration. The large ν_{CO} feature can be decomposed into three bands located at 1115, 1095, and 1055 cm^{-1}, in good agreement with those found earlier [27] at 1115, 1092, and 1060 cm^{-1}, respectively (Table 2).

On the basis of Table 2, the bands located at 1115 and 1095 cm^{-1} are assigned to dissociated methanol species, a monodentate methoxy (species I) and a bidentate methoxy

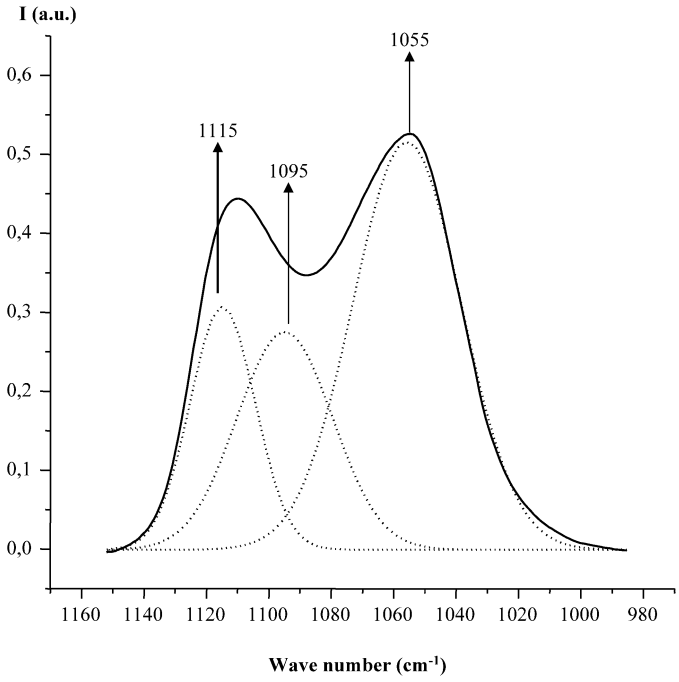

Fig. 6. FTIR spectrum obtained upon adsorption of methanol at room temperature (p_{MeOH} = 133 Pa) on MgO-hydration.

Table 2
Attribution of the ν_{CO} bands obtained by adsorption of methanol on MgO (adapted from [27])

ν_{CO} position (cm^{-1})	Attribution	Denomination
1060	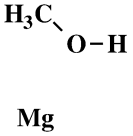	Species H
1092	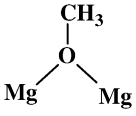	Species II
1115	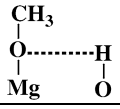	Species I

(species II), respectively. The band at 1055 cm^{-1} is assigned to molecularly adsorbed methanol involving H-bonding (species H).

Table 3 reports the areas of the three bands obtained for different MgO, along with the values obtained after hydration and subsequent evacuation at 673 K (except for MgO-CVD, for reasons of erosion, as explained in Section 3.4.2). The sums of the band areas corresponding to dissociated species are reported in the last column (the absorption coefficients of both species are assumed to be similar). The amount of dissociated methanol on surfaces dehydroxylated at 1023 K under vacuum increases in the order MgO-CVD < MgO-precipitation < MgO-hydration < MgO-sol–gel. On hydroxylated surfaces, the amount of dissociated methanol is less for all samples, suggesting that OH groups dissociate less methanol than O^{2-}_{LC} ions.

Table 3
Integrated area (normalized to 1 m^2 of surface area) of the three ν_{CO} bands obtained upon adsorption of methanol on clean or hydroxylated MgO surfaces

Sample	Pre-treatment	Integrated area of the band[a]			Sum of integrated areas of bands due to species I and II (dissociated CH_3OH)
		$\nu_I = 1115\ cm^{-1}$	$\nu_{II} = 1095\ cm^{-1}$	$\nu_H = 1060\ cm^{-1}$	
MgO-sol–gel	1023 K, vacuum	3.76	5.85	7.48	9.61
	H_2O, 673 K, vacuum	2.65	1.37	7.53	4.02
MgO-precipitation	1023 K, vacuum	4.77	1.00	10.68	5.77
	H_2O, 673 K, vacuum	2.94	0.83	11.18	3.77
MgO-hydration	1023 K, vacuum	2.85	3.74	7.93	6.59
	H_2O, 673 K, vacuum	2.76	2.05	7.69	4.81
MgO-CVD	1023 K, vacuum	0.94	1.70	3.16	2.64

[a] All the integrated areas are given in arbitrary units and come from the deconvolution of the ν_{CO} large contribution between 1000 and 1150 cm^{-1}.

4. Discussion

4.1. Thermodynamic Brønsted basicity versus reactivity of basic sites for clean surfaces

As was noted by Hattori [4], basic sites on MgO are usually obtained on thermal desorption of H_2O and CO_2, leading to surface reconstruction. It thus becomes difficult to compare the reactivity of the basic sites obtained [4,8,17]. Moreover, the influence of the remaining adsorbates in the vicinity of the liberated O^{2-}_{LC} ions cannot be neglected. To avoid this difficulty, different MgO samples were treated at high temperature (1273 K) to obtain stable surfaces involving different populations of O^{2-}_{LC} ions.

On thermal treatment of MgO, the more basic sites should be generated at higher temperatures after desorption of acidic molecules (CO_2, H_2O) [4,8]. So the stronger the interaction between the surface anion and the acidic molecule, the stronger the basic site from a thermodynamic standpoint. In this description, the basic sites are O^{2-}_{LC} ions, whose basicity is often related to their coordination [4,8]. As described earlier [28], different kinds of Mg–O pairs exist on MgO. O^{2-}_{LC} ions located at corners or edges of particles that adsorb CO_2, a Lewis acid, more strongly than O^{2-}_{5C} located on planes and than OH groups [8] thus can be considered the most basic Lewis sites from a thermodynamic standpoint.

The relative amount of dissociated methanol evaluated by IR (Table 3) is representative of the number of MgO pairs able to deprotonate methanol at ambient temperature. It is directly linked to the position of the following equilibrium (1), which can be considered an evaluation of the thermodynamic Brønsted basicity

$$CH_3OH + Mg^{2+}\,O^{2-} \rightleftharpoons \begin{bmatrix} O\,CH_3 & H \\ | & | \\ Mg & O \end{bmatrix}. \qquad (1)$$

It can be seen from Table 3 that the amount of dissociated methanol increases from MgO-CVD to MgO-sol–gel, with MgO-precipitation ≈ MgO-hydration being intermediate. Residual OH groups present on clean surfaces studied by adsorption of methanol may modify the O^{2-}_{3C}/O^{2-}_{4C} ratio reported in Table 1, because O^{2-}_{3C} ions are preferentially protonated [Bailly, in preparation]. However, it is very probable that the order given in Section 3.1 for the shift of the relative O^{2-}_{LC} distribution toward the less coordinated O^{2-}_{LC} ions is still representative of the state of clean surfaces considered here: MgO-CVD < MgO-hydration ≈ MgO-precipitation < MgO-sol–gel.

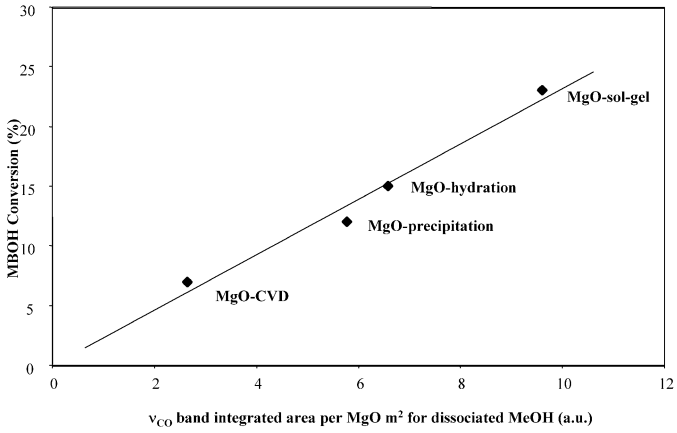

Fig. 7. Correlation, for different "clean" MgO surfaces, between MBOH conversion and thermodynamic Brønsted basicity evaluated from the integrated area of the ν_{CO} band per MgO m^2 for dissociated methanol.

Thus the dissociation of methanol appears to be favoured on O^{2-}_{LC} ions of lowest coordination number (3C better than 4C), in agreement with preliminary results obtained on the same samples, where the protonation of O^{2-}_{LC} ions with propyne is followed by photoluminescence [11]. This finding is also in agreement with theoretical calculations [29] showing that the deprotonation of methanol on MgO is enhanced in the presence of $O^{2-}_{3C,\,4C}$ ions.

The activity obtained in MBOH reaction depends on the nature of the surface. For clean surfaces, the order of activity is clearly correlated with thermodynamic Brønsted basicity evaluated for each sample (Fig. 7). The more the catalyst is able to dissociate methanol, the higher the activity, in agreement with the mechanistic route proposed for MBOH conversion on basic sites [17] (Fig. 8a). The first step involves the deprotonation of MBOH to form an alcoholate intermediate and an OH group. Thus the higher the coordination number of the MgO pairs involved, the lower the concentration of adsorbed alcoholate, resulting in a slowing of the kinetics of the following step.

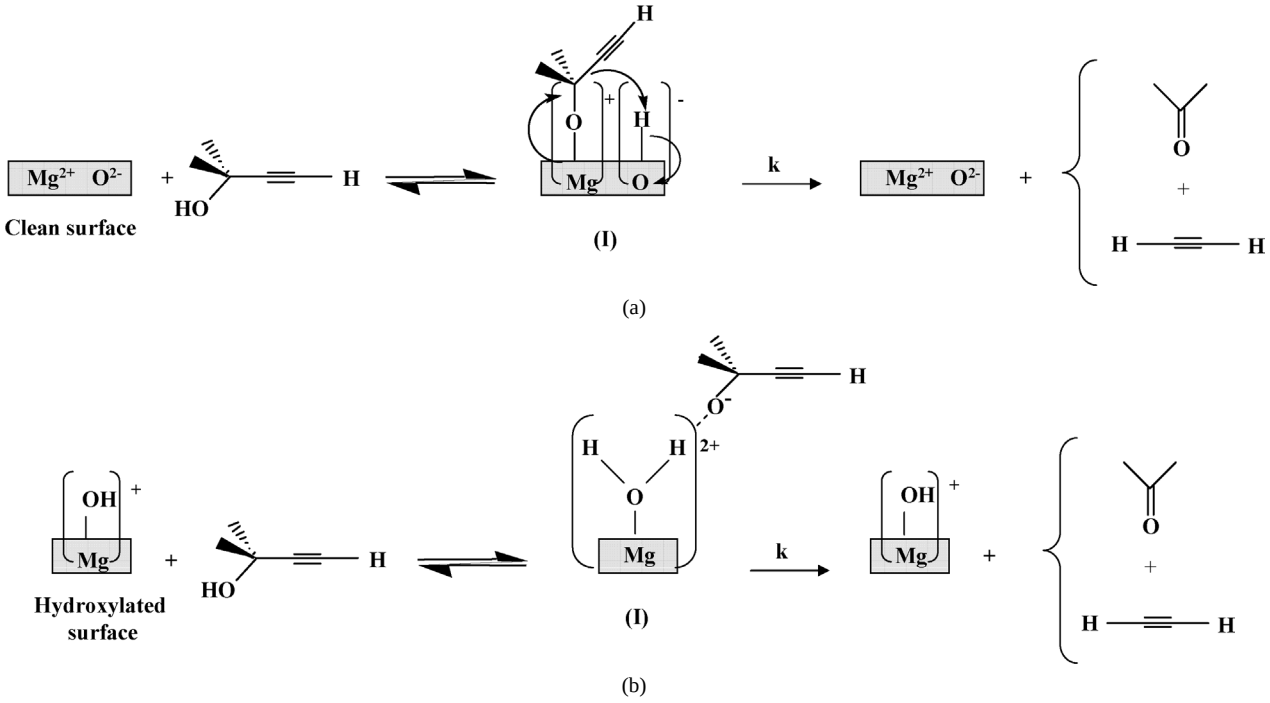

Fig. 8. (a) Mechanistic route for MBOH conversion into acetone and acetylene on a Mg^{2+} O^{2-} pair according to Ref. [17]. (b) Proposed mechanistic route for MBOH conversion into acetone and acetylene on hydroxyl groups, by analogy with the mechanism on clean surfaces (a).

4.2. Thermodynamic Brønsted basicity versus reactivity of basic sites for hydroxylated surfaces

To determine the influence of the nature of the sites on thermodynamic Brønsted basicity and on reactivity of basic sites, clean MgO surfaces have been hydroxylated and then evacuated at different temperatures. Thus the number and the nature of residual OH groups have been varied on each sample, and photoluminescence has been used to check whether the bands due to O^{2-}_{LC} ions are totally recovered after this hydration-dehydration sequence [10].

On the basis of IR-methanol experiments, it can be shown that hydroxylated surfaces deprotonate less methanol (Table 3), in agreement with the findings of Iizuka et al. [30], who studied the interaction of isopropanol and hydroxylated CaO. Thus the thermodynamic Brønsted basicity of OH groups seems lower than that of O^{2-}_{LC} ions, in agreement with the findings of Diez et al. [8] obtained from CO_2 TPD experiments.

In contrast, for MgO-precipitation (Fig. 5), MBOH conversion τ decreases with increasing temperature of evacuation, which removes OH groups and liberates Mg–O pairs. In that case, reactivity of basic sites is not correlated with thermodynamic Brønsted basicity of the surface. Such a discrepancy was observed by Xu et al. [31], who showed that CO_2 TPD, commonly used for measuring basic site density and strength, does not provide information on kinetically available basic sites. For example, these authors explained that strongly adsorbing sites are unlikely to participate in a catalytic reaction. They used experiments based on $^{13}CO_2/^{12}CO_2$ isotopic exchange to determine the amount of reversibly adsorbed CO_2 at the temperature of a given reaction. They then linked the constant rate of isotopic exchange to the reactivity of basic sites. In that case, of course, only Lewis basicity was probed, because no deprotonation step is implied in the CO_2 adsorption process.

For all samples, a good correlation was obtained between MBOH conversion τ and integrated area of the DRIFTS band (3700–3750 cm^{-1}) assigned to isolated OH groups [24]. From this correlation, it can be proposed that isolated OH groups are the active sites for converting MBOH into acetone and acetylene. This result suggests that OH groups, even though less basic than O^{2-}_{LC} ions, are more reactive.

4.3. Role of hydroxyl groups in the reactivity of basic sites

Such an enhancement of reactivity of basic sites on hydration has already been observed on MgO. For example, Zhang et al. [15] showed that the activity of the aldol condensation of acetone is increased when water is present and is not inhibited by CO_2 adsorption. They concluded that OH groups are the active sites because they weakly interact with CO_2 and are formed when water is introduced. Other examples include isopropanol decomposition and oxidative coupling of methane [32,33]. In the former case, OH groups are proposed to be the active sites; in the latter case, the enhancement of activity is related to the increase of basicity evidenced by a model reaction, the 2-butanol conversion. A good overview of the role played by basic OH groups in fine chemistry has been given by Climent et al. [34], who noted that in reactions like aldol and Claisen–Schmidt condensations, OH groups are the active sites even if they have a medium basic strength. These effects have been observed on hydrotalcite materials, as reported by Rao et al. [35] and Prinetto et al. [36].

As for MBOH conversion, the influence of the nature of the basic sites has not been investigated, although very good

correlations have been found between thermodynamic basicity and activity of basic sites [6,37], as evidenced here for clean MgO surfaces. Nevertheless, Constantino and Pinnavaia [38] observed that hydrotalcites activated below the decomposition temperature (<523 K) are more active than the resulting amorphous oxides. The possible intercalation of MBOH between the layers of the material was suggested as an explanation for its high activity. We can now propose that instead, the MBOH reactivity is due to OH groups, as has been observed on hydrotalcites for condensation reactions [34–36,39].

4.4. Proposed mechanism for the conversion of MBOH

To explain the activity of MBOH conversion, let us consider the mechanism proposed in Fig. 8a. The rate of formation of the products can be written as $r = k\theta_{\mathrm{I}}$, where k is the rate constant of the second step and θ_{I} is the coverage of the surface by the alcoholate intermediate (I).

Because θ_{I} is directly linked to the thermodynamic constant of the first equilibrium, the concentration of alcoholate increases with the deprotonating strength of the Mg–O pair. At the same time, the alcoholate intermediate is more stable: its reactivity implies the release of the proton located on O^{2-}_{LC} ion and the back-donation of electrons stabilized by the Lewis acid site, which is more difficult with an acid–base pair with high deprotonating ability. Thus k is expected to decrease with increasing thermodynamic Brønsted basicity.

In the case of clean surfaces, these two antagonist effects result in a good correlation between thermodynamic Brønsted basicity and reaction rate. The higher the concentration of O^{2-}_{LC}, the more active the catalyst. In contrast, it has been shown that the thermodynamic Brønsted basicity of the surface is decreased on hydroxylation. The coverage is thus lower in alcoholate intermediate θ_{I} than on the clean surface. However, as shown in Fig. 8b, the deprotonation of an alcohol such as MBOH on a basic OH group forms a likely very reactive alcoholate, because it is stabilized on a poor Lewis site, $[Mg(OH)_2]^{2+}$. So the high reactivity of basic OH groups can be assigned to the Sabatier principle [40], which states that to be active, a catalyst must adsorb the reactant to give an unstable temporary intermediate that can further evolve on the surface to finally lead to the product that desorbs. It should be noted that the mechanism shown in Fig. 8b is tentatively proposed by analogy with the mechanistic route on clean surfaces (Fig. 8a). Further studies to validate this are currently underway.

5. Conclusion

MgO samples with different morphologies were prepared and classified according to the relative distribution of O^{2-}_{LC} ions of varying coordination, determined from photoluminescence spectra [12]. The relative distribution of O^{2-}_{LC} ions (where LC = 3C, 4C, and 5C refer to tri-, tetra-, and penta-coordinated oxide ions, respectively) is shifted toward the less coordinated ions along the series MgO-CVD < MgO-hydration ≈ MgO-precipitation < MgO-sol–gel.

Preparation of clean surfaces, obtained after removal of carbonates and OH groups by thermal treatment above 1023 K, allowed us to evaluate the influence of the coordination of basic O^{2-}_{LC} ions on the basic properties of the surfaces. These surfaces transform MBOH according to its basic route, leading to acetone and acetylene in an equimolar ratio. The comparison of the conversion level measured in isosurface area conditions gives the following order of activity of basic sites: MgO-CVD < MgO-precipitation < MgO-hydration < MgO-sol–gel, suggesting that the lower the coordination of O^{2-}_{LC} ions, the greater the reactivity of basic sites.

Hydroxylation of the surface performed by hydration of clean surfaces results in the enhancement of reactivity of basic sites, although basic O^{2-}_{LC} ions of lower coordination are covered by protons. This infers that OH groups are also directly implied in the reactivity of basic sites, as confirmed by the correlation between the number of isolated OH groups and the MBOH conversion level. Thus, depending on the hydroxylation state of the surface, some basic O^{2-}_{LC} sites may be poisoned by protons, but the number of active basic sites is maintained constant, because other basic sites (OH groups), even more reactive than O^{2-}_{LC}, are generated on water dissociation.

Because the reactivity of basic sites, leading to an anionic intermediate [4], implies a deprotonation step, we studied the relationship between reactivity of basic sites and deprotonation ability of Brønsted basic sites present on clean and hydroxylated surfaces. The position of the deprotonation equilibrium of a protic acidic molecule, such as methanol reacting with MgO, determines the thermodynamic Brønsted basicity of MgO surfaces. The ability of the latter to deprotonate methanol was evaluated by in situ transmission IR and a classification was established by comparing the integrated areas of the ν_{CO} bands related to dissociated methanol. For clean surfaces, the lower the coordination of O^{2-}_{LC}, the higher the deprotonation ability, indicating a correlation between the latter and the reactivity of basic sites. Hydroxylation of surfaces results in decreased deprotonation ability, indicating that OH groups are less deprotonating than O^{2-}_{LC}. But despite of their lower deprotonation ability, OH groups are very reactive; the lower coverage of alcoholate intermediate on hydroxylated surfaces is compensated by its higher reactivity. Indeed, the $O_{LC}H$ groups formed during deprotonation on clean surfaces are particularly stable.

Further studies combining experimental and theoretical methods are in progress to improve our understanding of the exact nature of active OH groups and of the reaction mechanism.

Acknowledgments

The authors wish to express their sincere gratitude to Dr. Ph. Bazin from Laboratoire de Catalyse et Spectrochimie, CNRS-ENSICAEN, University of Caen (France) for his help in performing the methanol-IR experiments and to Drs. J.C. Lavalley and J. Saussey from the same laboratory for very fruitful discussions. They also thank Professor E. Knözinger of the University of Wien for kindly providing the MgO-CVD sample.

References

[1] K. Tanabe, W.F. Hölderich, Appl. Catal. 181 (1999) 399.
[2] H. Pines, W.M. Stalick, Base-Catalyzed Reactions of Hydrocarbons and Related Compounds, Academic Press, New York, 1977.
[3] Y. Ono, J. Catal. 216 (2003) 406.
[4] H. Hattori, Appl. Catal. A 222 (2001) 247.
[5] J.M. Fraile, J.I. Garcia, J.A. Mayoral, Catal. Today 57 (2000) 3.
[6] U. Meyer, W.F. Hoelderich, J. Mol. Catal. A 142 (1999) 213.
[7] J.C. Lavalley, Catal. Today 27 (1996) 377.
[8] V.K. Díez, C.R. Apesteguía, J.I. Di Cosimo, Catal. Today 63 (2000) 53.
[9] J.N. Brønsted, Rec. Trav. Chim. Pays-Bas 42 (1923) 718.
[10] M.L. Bailly, PhD thesis, Université Pierre et Marie Curie, Paris, 2003.
[11] M.L. Bailly, G. Costentin, J.M. Krafft, M. Che, Catal. Lett. 92 (2004) 101.
[12] M.L. Bailly, G. Costentin, H. Lauron-Pernot, J.M. Krafft, M. Che, J. Phys. Chem. B 109 (2005) 2404.
[13] M. Che, A.J. Tench, Adv. Catal. 31 (1982) 77, AERE Report – R 9971 nov 1980.
[14] M. Anpo, M. Che, Adv. Catal. 44 (1999) 119.
[15] G. Zhang, H. Hattori, K. Tanabe, Appl. Catal. 36 (1988) 189.
[16] F. Hoq, I. Nieves, K.J. Klabunde, J. Catal. 123 (1990) 349.
[17] H. Lauron-Pernot, F. Luck, J.M. Popa, Appl. Catal. 78 (1991) 213.
[18] A. Becker, S. Benfer, P. Hofmann, K.H. Jacob, E. Knözinger, Ber. Bunsen-Ges. Phys. Chem. 99 (1995) 1328.
[19] E. Knözinger, O. Diwald, M. Sterrer, J. Mol. Catal. A 162 (2000) 83.
[20] H. Thorms, M. Epple, H. Viebrock, A. Reller, J. Mater. Chem. 5 (1995) 589.
[21] S. Coluccia, A.J. Tench, R.L. Segall, J. Chem. Soc., Faraday Trans. 1 75 (1979) 1769.
[22] M. Anpo, Y. Yamada, Mater. Chem. Phys. 18 (1988) 445.
[23] S. Coluccia, L. Marchese, S. Lavagnino, M. Anpo, Spectrochim. Acta A 43 (1987) 1573.
[24] E. Knözinger, K.H. Jacob, S. Singh, P. Hofmann, Surf. Sci. 290 (1993) 388.
[25] P.J. Anderson, P.J. Horlock, J.F. Oliver, Trans. Faraday Soc. 61 (1965) 2754.
[26] A.J. Tench, D. Giles, J.F.J. Kibblewhite, Trans. Faraday Soc. 67 (1971) 854.
[27] M. Bensitel, O. Saur, J.C. Lavalley, Mater. Chem. Phys. 28 (1991) 309.
[28] S. Coluccia, A.J. Tench, Stud. Surf. Sci. Catal. 7B (1981) 1154.
[29] C. Di Valentin, A. Del Vitto, G. Pacchioni, S. Abbet, A.S. Wörz, K. Judaï, U. Heiz, J. Phys. Chem. B 106 (2002) 11961.
[30] T. Iizuka, H. Hattori, Y. Ohno, J. Sohma, K. Tanabe, J. Catal. 22 (1971) 130.
[31] M. Xu, M.J.L. Gines, A.-M. Hilmen, B.L. Stephens, E. Iglesia, J. Catal. 171 (1997) 130.
[32] S. Kus, M. Otremba, A. Tórz, M. Taniewski, Fuel 81 (2002) 1755.
[33] J.A. Wang, X. Bokhimi, O. Novaro, T. López, R. Gómez, J. Mol. Catal. 145 (1999) 291.
[34] M.J. Climent, A. Corma, S. Iborra, A. Velty, J. Mol. Catal. A 182–183 (2002) 327.
[35] K.K. Rao, M. Gravelle, J. Sanchez Valente, F. Figueras, J. Catal. 173 (1998) 115.
[36] F. Prinetto, D. Tichit, R. Teissier, B. Coq, Catal. Today 55 (2000) 103.
[37] (a) M.A. Aramendia, V. Borau, C. Jiménez, J.M. Marinas, A. Marinas, A. Porras, F.J. Urbano, J. Catal. 183 (1999) 240;
(b) M.A. Aramendia, V. Borau, I.M. Garcia, C. Jiménez, A. Marinas, J.M. Marinas, A. Porras, F.J. Urbano, Appl. Catal. A 184 (1999) 115.
[38] (a) V.R.L. Constantino, T.J. Pinnavaia, Catal. Letters 23 (1994) 361;
(b) V.R.L. Constantino, T.J. Pinnavaia, Inorg. Chem. 34 (1995) 883.
[39] M.J. Climent, A. Corma, S. Iborra, K. Epping, A. Velty, J. Catal. A 225 (2004) 316.
[40] P. Sabatier, in: Ch. Béranger (Ed.), La Catalyse en Chimie Organique, Librairie Polytechnique, 2ème édition, Paris, Liège, 1920, p. 65.